2021 43rd Annual International Conference of the
IEEE Engineering in Medicine & Biology Society (EMBC)
Oct 31 - Nov 4, 2021. Virtual Conference

A visualization tool for assessment of spinal cord functional magnetic resonance imaging data quality*

Kimberly J. Hemmerling and Molly G. Bright

Abstract— **Functional magnetic resonance imaging (fMRI) is an extensively used neuroimaging technique to non-invasively detect neural activity. Data quality is highly variable, and fMRI analysis typically consists of a number of complex processing steps. It is crucial to visually assess images throughout analysis to ensure that data quality at each step is satisfactory. For fMRI analysis of the brain, there is a simple tool to visualize four-dimensional data on a two-dimensional plot for qualitative analysis. Despite the practicality of this method, it cannot be directly applied to fMRI data of the spinal cord, and a comparable approach does not exist for spinal cord fMRI analysis. The additional challenges encountered in spinal cord imaging, including the small size of the cord and the influence of physiological noise sources, drive the importance of developing a similar visualization technique for spinal cord fMRI. Here, we introduce a highly versatile image analysis tool to visualize spinal cord fMRI data as a simple heatmap and to co-visualize relevant traces such as physiological or motion timeseries. We present multiple variations of the plot, data features that can be identified with the heatmap, and examples of the useful qualitative analyses that can be performed using this method. The spinal cord plot can be easily integrated into an fMRI analysis pipeline and can streamline visual inspection and qualitative analysis of functional imaging data.**

Clinical Relevance— **Implementation of this data visualization method is a simple addition to spinal cord fMRI analysis that could be used to identify normal vs. abnormal signal variation in pathologies that impact the cord, such as spinal cord injury or multiple sclerosis.**

I. Introduction

Functional magnetic resonance imaging (fMRI) is widely used as a non-invasive method to detect neural activity in the central nervous system. Blood-oxygenation level dependent (BOLD) contrast is a standard mechanism for detection of neural activity in fMRI and is based on neurovascular coupling: it relies on the change in blood flow and blood oxygenation that is the local hemodynamic response to increased neural activity [1-2]. Specifically, the change in relative concentrations of deoxygenated and oxygenated blood influence local T2* relaxation times, resulting in changes to the BOLD-weighted fMRI signal [2]. fMRI can be used to assess the health and function of the central nervous system by characterizing the response to a task or stimulus, or by measuring resting state activity.

Although fMRI can provide valuable insights, there are still many challenges pertaining to data quality, noise, and artifacts. A technique developed for brain imaging visualizes fMRI data as a two-dimensional grayscale heatmap; timeseries from brain tissues are plotted vertically from superficial gray matter to deeper cerebrospinal fluid (CSF) in the ventricles [3]. Additionally, in close proximity to these plots are traces such as those from head motion or a respiratory belt, used to visually identify any coincidence of signal variation and artifacts in the scan [3]. The fMRI community has realized the utility of these plots and analyzed BOLD signal changes with respect to head motion [4], for quality control [5-6], and compared data denoising approaches [7]. The integration of this visualization into analyses can greatly improve the holistic impression of fMRI data in the brain, qualitatively capturing the impact of artifacts, movement, and other contributors to scan quality.

Although this technique is highly useful for brain imaging, it cannot currently be applied to spinal cord imaging data. Anatomical properties of the spinal cord cause imaging this region to be particularly difficult. Specifically, the cross-sectional diameter of the spinal cord is approximately 8–12mm in the cervical cord, requiring high spatial resolution during scanning [8]. The small size leads to an increased likelihood of partial volume effects in voxels that cross boundaries of gray matter, white matter, or CSF. The tissues in and around the cord also differ in magnetic susceptibility, causing inhomogeneities in the static magnetic field and signal disruptions [8-9]. Furthermore, there are major noise contributions from physiological sources that are more severe than in brain imaging. Respiration leads to movement of the spinal cord throughout the breathing cycle; the cardiac cycle causes pulsatile movement of the CSF surrounding the cord, as well as in the nearby vasculature [8].

These additional challenges in spinal cord fMRI increase the motivation to visualize these data on two-dimensional heatmaps similar to those regularly used in brain data. Unfortunately, due to the specificity of software to the anatomy being imaged, such as the use of Freesurfer to segment brain tissues [3], the current method cannot be directly applied to the spinal cord. Another difficulty is that the organizational priorities for sorting data along the vertical axis of the heatmap may differ in the spinal cord compared to the brain because of the differing functional anatomy. In this paper, we present a method for visualization of four-dimensional spinal cord fMRI data that can be easily implemented into a preprocessing pipeline for data quality analysis. Additionally, we show examples of how the spinal cord plot can be reorganized and utilized to assess noise and artifacts.

*Research supported by the Craig H. Neilsen Foundation (595499).

K. J. Hemmerling and M. G. Bright are with the Department of Biomedical Engineering and the Department of Physical Therapy & Human Movement Sciences, Northwestern University, Chicago, IL 60611 USA (email: khemmerling@northwestern.edu; molly.bright@northwestern.edu).

II. Methods

This study was approved by the Northwestern University Institutional Review Board, and all participants gave written informed consent. The T2*-weighted fMRI data were acquired at the cervical spine with gradient-echo echo-planar imaging sequences and ZOOMit selective excitation (TE=30ms, TR=2s, 1x1x3mm^3). Data were either resting-state scans or breathing task scans, during which participants completed a sequence of regularly spaced breath-holds. The chosen example data specifically show some artifact or feature that explains the utility of this visualization technique. Prior to visualization all data were minimally preprocessed. Data were motion corrected with the Spinal Cord Toolbox function *sct_fmri_moco* [10], then registered to the PAM50 template space [11].

A. Organization of spinal cord data

Template PAM50 masks of the spinal cord, vertebral levels, gray matter, white matter, and CSF transformed to the functional space are used to organize the heatmap data according to two separate schemes: tissue type and vertebral level. *Tissue Type:* The first organizational method attempts to differentiate deep gray matter to superficial white matter signals. Due to partial volume effects, the outermost voxels are expected to also contain signal from CSF around the cord. Binarized versions of the white and gray matter masks are iteratively eroded and subtracted to create concentric masks of the spinal cord (Fig. 1A). Optionally, CSF masks could also be created in this step, but are not shown here because those voxels would become the majority of the plot, and the gray and white matter signal are typically of greater interest in fMRI data analyses. Within each tissue mask, the data are also sorted by slice; superior to inferior data are plotted from top to bottom. *Vertebral Level:* The second method was generated to consider how artifacts may vary along the longitudinal axis of the cord and directly implements the transformed PAM50 vertebral level mask to sort the data by vertebral level and slice (Fig. 1B). For both methods, the timeseries data for each voxel within these masks are exported and stored.

These steps are compiled in a shell script which integrates functions from the Spinal Cord Toolbox [10], FSL [12], and AFNI [13], and can process spinal cord fMRI data that has been registered to the PAM50 template.

B. The spinal cord plot visualization

The fMRI timeseries from the masks are organized on the vertical axis according to the user's input (Fig. 1). The most basic version of the plot includes just the functional data and a colorbar. Colorbars plotted to the left of each heatmap indicate which organizational method is being used and where in the cord those voxels are located. Additional output plots are dependent on the user's input and choices.

If physiological, motion, or other traces are provided, data are also co-visualized with those relevant traces. Physiological traces may include end-tidal CO_2 ($P_{ET}CO_2$), end-tidal O_2, heart rate (HR), or respiratory belt data, and are visualized above the heatmap. Motion traces, such as the estimates output from an inter-volume registration algorithm, are also presented below the plot. A generalized linear model (GLM) is performed using a design matrix of the task, physiological noise, and/or motion

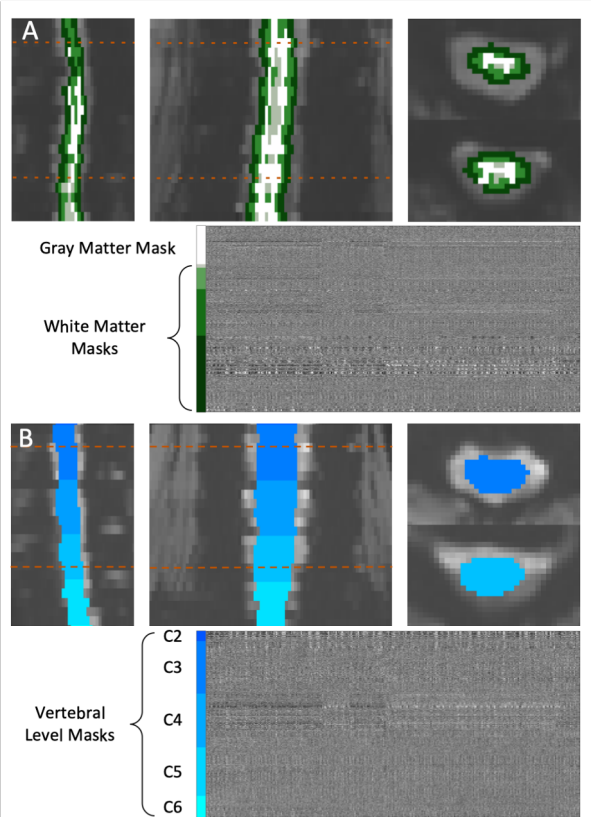

Figure 1. The two organizational methods for the heatmaps based on spinal cord anatomy shown on a 6.8-minute resting state functional scan. **(A)** The tissue type organization uses concentric masks of the spinal cord gray matter, indicated by the white mask, and of the white matter, indicated by the gray and green masks. Nested within each of those masks, the data are additionally sorted by slice. An example heatmap organized by tissue type is shown. **(B)** The vertebral level method is organized by level and slice. The shades of blue indicate the cervical vertebral levels included in this dataset. An example heatmap organized by vertebral level is shown.

traces, and voxelwise t-statistics are calculated for each model regressor. The heatmap, t-statistics, and regressors are all plotted to further visualize the contributions of relevant traces. The heatmap can also be reorganized according to the magnitude of specific t-statistics. Additionally, the frequency content of the fMRI data and all regressors can be visualized via plots of the relevant power spectra. In each of these figures, the heatmaps and traces are temporally lined up to enable visual discernment of the coincidence of data variation. A MATLAB (MathWorks, Natick, MA) function accepts the sorted timeseries as input data and performs these steps to create the desired heatmaps. The user can decide which data to input and which of the data visualizations they desire as output. Additional output from the function includes a directory of voxel coordinates (including the vertebral level if that organization was used) corresponding to the heatmap.

III. Results & Discussion

The heatmap organization – by tissue type or by vertebral level – can be switched to compare between the two methods, revealing interesting structured variance in spinal cord fMRI data. Examples of tissue type and vertebral level organizations are presented for a resting-state spinal cord fMRI dataset (Fig.

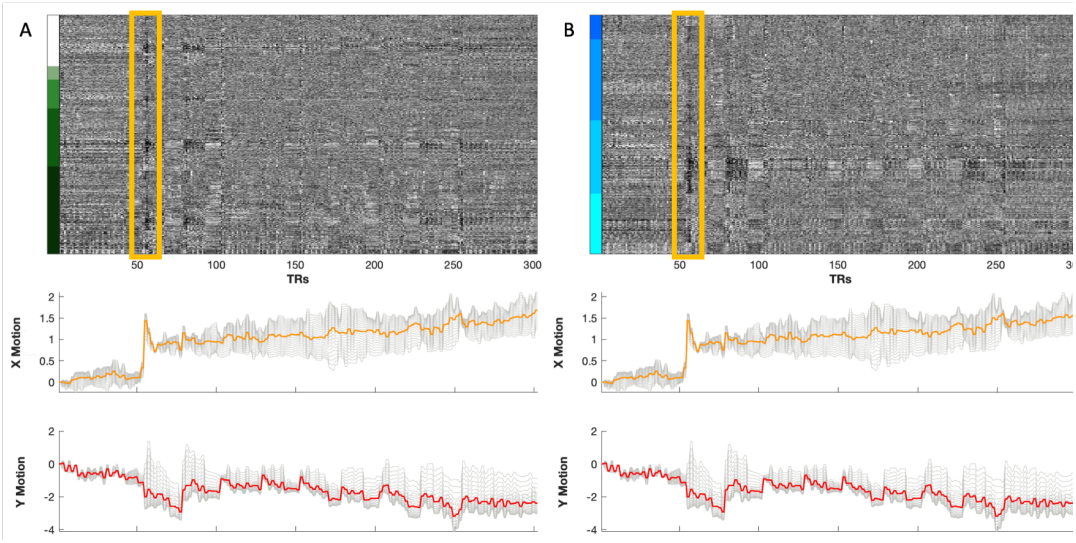

Figure 2. Heatmaps of a breath-hold scan presented with X and Y motion traces organized by both tissue type and by vertebral level. The slicewise X and Y motion traces are represented by light gray lines, and their average is represented by the orange and red lines, respectively. **(A)** The tissue type organization of the heatmap has a distinct signal artifact at approximately TR=50 seconds (yellow box), and the X and Y motion traces both have an abrupt movement at the same point in time. **(B)** The vertebral level organization of the same dataset shows the same abrupt motion artifact, but this heatmap organization rearranges the data so that the signal variation is more concentrated in the lower vertebral levels, indicating differential effects of the motion along the longitudinal axis of the body and spinal cord.

1). In both versions of this heatmap, there is some visible structured signal variance. In the tissue type organization (Fig. 1A), this variation appears to be spread throughout the gray matter and white matter tissue classes, although potentially most visible in the outermost white matter voxels (nearest to the CSF). In the vertebral level organization (Fig. 1B), the variation appears most prominently in the C2 and C4 vertebral levels. These multiple organizations are useful for determining the spatial distribution of signal variance, which may add insight into the source and impact of these effects.

Fig. 2 uses an example spinal cord breath-hold task fMRI dataset to demonstrate how artifacts visualized with our approach can enable the user to identify signal variation that may be attributable to movement. Motion parameters from the Spinal Cord Toolbox algorithm that estimates and corrects for in-plane translations are shown below the heatmap. X and Y motion describe left-right and dorsal-ventral motion, respectively. In the fMRI data, there is a distinct signal artifact indicated by the boxed area. There is a concurrent spinal cord movement in both the X and Y motion traces, and most predominantly in the X Motion trace. In the tissue type organization of this plot, the signal artifact appears to be spread throughout tissue classes, without any regional specificity (Fig. 2A). However, the vertebral level organization of the same data shows that most of the signal artifact is located in the lower vertebral levels, suggesting that the artifact reflects participant movement of the more rostral portion of their cervical spinal cord (Fig. 2B).

Fig. 3 shows spinal cord fMRI data from a scan intended to measure vascular reactivity via changes to arterial CO_2 induced with a repeated breath-hold task [1]. $P_{ET}CO_2$ and HR are two of the physiological traces that were measured during this scan, and their demeaned traces convolved with the hemodynamic and cardiac response functions, respectively, are above the heatmap. The traces from motion correction for this scan are visualized below the plot. Positioned to the right of the heatmap are the magnitude of the t-statistics derived from GLM fitting (with the color corresponding to the pertinent regressor plot), and can be used to visualize how the regressors account for variation in the functional data. The brightness of these t-statistics indicates the strength of the parameter estimate for that voxel. The structured variation in

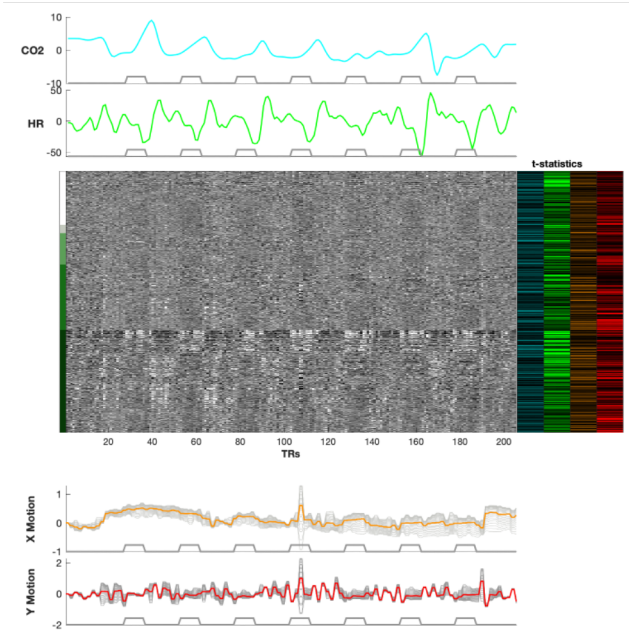

Figure 3. A heatmap organized by tissue type, co-visualized with the physiological and motion regressors used in a generalized linear model. The timing of the repeated breath-hold task used during this functional scan is shown in each subplot. The slicewise X and Y motion traces are represented by light gray lines, and their average is represented by the orange and red lines, respectively. The voxelwise t-statistics of the model fits are presented to the right of the heatmap.

this heatmap appears as periodic, wide vertical bands that seem to coincide temporally with HR fluctuations, as well as with some of the fluctuation in $P_{ET}CO_2$. The bright color across the HR t-statistics bar implies the strength of the model fit of this regressor, though this effect is difficult to interpret due to possible collinearity between the HR and $P_{ET}CO_2$ regressors. The direct intention of the breath-holding task is the manipulation of $P_{ET}CO_2$, but this plot highlights the challenge of covariance between that and other regressors in the GLM.

In scans with periodic signals or task designs, like that represented in Fig. 3, the frequency content of the BOLD fMRI timeseries may also be of interest. Fig. 4 shows the power spectra of the physiological signals and fMRI timeseries of the same breath-hold scan. By visualizing the data this way, it is clear that both CO_2 and HR have a dominant frequency peak at approximately 0.02 Hz, which corresponds to the brightest band in the frequency heatmap, as indicated by the arrows. There are additional bands at higher frequencies that correspond to the harmonics of the task paradigm.

As shown, we can use this spinal cord plot to visualize a variety of fMRI scans, artifacts, and data features. Along with the tissue type organization, similar to what is used for the brain imaging plot [3], the addition of the vertebral level method is key because each uniquely considers ways in which noise and artifacts may impact spinal cord fMRI. We have seen how data structure and variation depend on these two methods. We have demonstrated motion coinciding with signal variance and how this holistic visualization of data can highlight covariance between GLM regressors. Our method provides a simplification of data quality inspection.

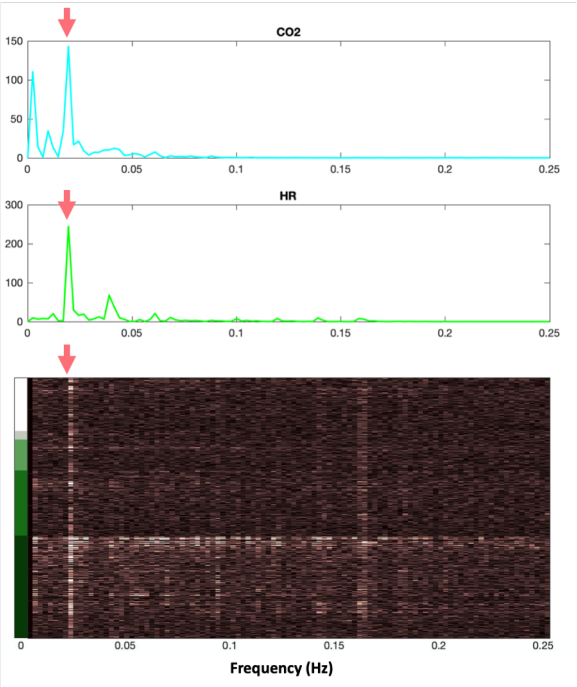

Figure 4. The power spectra of the same breath-hold task scan, end-tidal CO_2, and heart rate traces shown in Fig. 3. All are limited by the Nyquist frequency. Similar frequency peaks are seen in the physiological traces and the frequency heatmap, as indicated by the arrows. Additional frequency bands correspond to the harmonics of the breath-hold task stimulus timings.

IV. Conclusion

We have presented a non-exhaustive selection of the visualization options using our spinal cord fMRI heatmap technique. Each variation is a valuable approach to analyze imaging data and their correspondence to other signals prior to further processing and statistical analysis. This tool can be applied to quickly compare different datasets to each other or to compare one dataset at each step in a preprocessing pipeline.

Appendix

Code, instructions, and example data that may be used to try out this visualization tool are available on GitHub: https://github.com/BrightLab-ANVIL/spinalcordplot.

Acknowledgements

We thank Dr. Mark Hoggarth, Dr. Rachael Stickland, and Apoorva Ayyagari for the collection of imaging data. Data were collected at the Center for Translational Imaging (CTI) in the Department of Radiology at the Northwestern University Feinberg School of Medicine, and we thank Rachael Young, Dr. Todd Parrish, and Dr. Yufen Chen at the CTI for their contributions to data collection.

References

[1] J. Pinto, M. G. Bright, D. P. Bulte, and P. Figueiredo, "Cerebrovascular Reactivity Mapping Without Gas Challenges: A Methodological Guide," *Front. Physiol.*, vol. 11, pp. 1–19, Jan. 2021.

[2] E. M. C. Hillman, "Coupling mechanism and significance of the BOLD signal: a status report," *Annu. Rev. Neurosci.*, vol. 37, pp. 161–181, 2014.

[3] J. D. Power, "A simple but useful way to assess fMRI scan qualities," *Neuroimage*, vol. 154, pp. 150–158, Jul. 2017.

[4] C. Gratton *et al.*, "Removal of high frequency contamination from motion estimates in single-band fMRI saves data without biasing functional connectivity," *Neuroimage*, vol. 217:116866, Aug. 2020.

[5] D. A. Fair *et al.*, "Correction of respiratory artifacts in MRI head motion estimates," *Neuroimage*, vol. 208:116400, Mar. 2020.

[6] J. Li *et al.*, "Global signal regression strengthens association between resting-state functional connectivity and behavior," *Neuroimage*, vol. 196, pp. 126–141, Aug. 2019.

[7] M. F. Glasser *et al.*, "Using temporal ICA to selectively remove global noise while preserving global signal in functional MRI data," *Neuroimage*, vol. 181, pp. 692–717, Nov. 2018.

[8] F. Eippert, Y. Kong, M. Jenkinson, I. Tracey, and J. C. W. Brooks, "Denoising spinal cord fMRI data: Approaches to acquisition and analysis," *Neuroimage*, vol. 154, pp. 255–266, Jul. 2017.

[9] Y. Kong, M. Jenkinson, J. Andersson, I. Tracey, and J. C. W. Brooks, "Assessment of physiological noise modelling methods for functional imaging of the spinal cord," *Neuroimage*, vol. 60, no. 2, pp. 1538–1549, Apr. 2012.

[10] B. De Leener *et al.*, "SCT: Spinal Cord Toolbox, an open-source software for processing spinal cord MRI data," *Neuroimage*, vol. 145, pp. 24–43, Jan. 2017.

[11] B. De Leener, V. S. Fonov, D. L. Collins, V. Callot, N. Stikov, and J. Cohen-Adad, "PAM50: Unbiased multimodal template of the brainstem and spinal cord aligned with the ICBM152 space," *Neuroimage*, vol. 165, pp. 170–179, Jan. 2018.

[12] M. Jenkinson, C. F. Beckmann, T. E. J. Behrens, M. W. Woolrich, and S. M. Smith, "FSL.," *Neuroimage*, vol. 62, no. 2, pp. 782–90, Aug. 2012.

[13] R. W. Cox and J. S. Hyde, "Software tools for analysis and visualization of fMRI data," *NMR Biomed.*, vol. 10, no. 4–5, pp. 171–178, Jun. 1997.